ARTICLE

Stacking Interactions of Resonance-Assisted Hydrogen-Bridged Rings and C_6-Aromatic Rings

Received 00th January 20xx,
Accepted 00th January 20xx

DOI: 10.1039/x0xx00000x

Jelena P. Blagojević Filipović, [a] Michael B. Hall [b] and Snežana D. Zarić * [c,d]

Stacking interactions between six-membered resonance-assisted hydrogen-bridged rings (RAHB) and C_6-aromatic rings are systematically studied by analyzing crystal structures in Cambridge Structural Database (CSD). The interaction energies were calculated by quantum-chemical methods. Although the interactions are stronger than benzene/benzene stacking interactions (-2.7 kcal/mol) the strongest calculated RAHB/benzene stacking interaction (-3.7 kcal/mol) is significantly weaker than the strongest calculated RAHB/RAHB stacking interaction (-4.7 kcal/mol), but for particular composition of RAHB rings RAHB/benzene stacking interactions can be weaker or stronger than the corresponding RAHB/RAHB stacking interactions. They are also weaker than the strongest calculated stacking interaction between five-membered saturated hydrogen-bridged rings and benzene (-4.4 kcal/mol) and between two five-membered saturated hydrogen-bridged rings (-4.9 kcal/mol). SAPT energy decomposition analyses show that the strongest attractive term in RAHB/benzene stacking interactions is dispersion, however, it is mostly canceled by repulsive exchange term, hence the geometries of the most stable structures are determined by electrostatic term.

Introduction

The stacking interactions are mainly connected with aromatic molecules,[1-10] however it was shown that various rings can form stacking interactions; aliphatic saturated[11-16] and unsaturated molecules,[17,18] metal-chelate rings,[19-38] and hydrogen-bridged rings.[39-42] 2D materials can also form stacking interactions.[43-46] Cyclic hydrocarbons of similar size, benzene and cyclohexane, have similar stacking energies in dimer structures, -2.73 kcal/mol[47] and -2.62 kcal/mol,[48] respectively. Differences in the binding strength of the small aromatic and saturated hydrocarbon dimers in stacked geometry are not large, but they become significant with increasing system size.[11] A cyclohexane/benzene system is even more stable in stacked arrangement (-3.27 kcal/mol)[12] than benzene/benzene and cyclohexane/cyclohexane dimers. The calculated optimal geometry in cyclohexane/benzene system is parallel-displaced, as in benzene dimer. Stacked structures of phenyl and cyclohexyl groups are also significantly present in crystals that contain these fragments. The arrangement in crystal structures is parallel-displaced, which is in accordance with the quantum chemical calculations.[12]

Square-planar metal-chelate rings in crystal structures can form stacking interactions mutually[19,23-27,32-35] and with aromatic rings.[19,21,28,32,33] Quantum chemical calculations of interaction energies show that the chelate/chelate stacking interactions (up to -10.34 kcal/mol)[19,33], are stronger than chelate/benzene interactions (up to -7.52 kcal/mol),[19,32,33] while both of them are stronger than benzene/benzene stacking (-2.73 kcal/mol).[47]

Hydrogen-bridged rings are observed to form CH/π interactions like the rings formed only by covalent bonding.[37,49] The formation of hydrogen-bridged ring stacking interactions is found by systematic analyses of structures from Cambridge Structural Database (CSD) and interaction energies were calculated by quantum chemical methods on model systems.[39-41] The contribution of parallel contacts in the total number of contacts involving hydrogen bridged rings is considerable; 86% of all contacts between planar saturated five-membered hydrogen-bridged rings (an example of these species is given in Figure 1a) are parallel contacts,[39] 45% of all contacts involving planar saturated five-membered hydrogen-bridged rings form parallel contacts with C_6-aromatic group,[40] while 91% of all contacts between six-membered resonance-assisted hydrogen-bridged (RAHB) rings (an example is given in Figure 1b) are in mutual parallel orientations.[41] The most stable obtained dimer geometries are mainly parallel-displaced, as in benzene dimer, however, the interactions are stronger. The strongest calculated energy of stacking interactions between two saturated hydrogen-bridged rings is

[a] Innovation Center of the Faculty of Chemistry, Studentski trg 12-16, Belgrade, Serbia.
[b] Department of Chemistry, Texas A&M University, College Station, TX 77843-3255, USA.
[c] Faculty of Chemistry, University of Belgrade, Studentski trg 12-16, Belgrade, Serbia.
[d] Department of Chemistry, Texas A&M University at Qatar, P. O. Box 23874, Doha, Qatar

Electronic Supplementary Information (ESI) available: Additional analyses of the geometrical parameters from CSD, evaluation of quantum-chemical methods, additional calculations. See DOI: 10.1039/x0xx00000x

-4.89 kcal/mol,[39] -4.38 kcal/mol of a saturated hydrogen bridge ring/benzene system[40] and -4.76 kcal/mol of a RAHB dimer,[41] while the interaction in stacked benzene dimer is -2.73 kcal/mol.[47] It can be noticed that the presence of a conjugated double bonds system in RAHB does not have much influence on the interaction strength.[41]

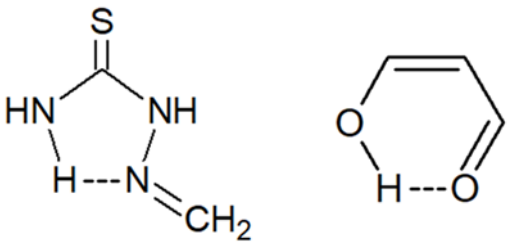

a) b)

Figure 1. Examples of molecules that were used previously for studying the stacking interactions of hydrogen-bridged rings a) a saturated hydrogen-bridged ring (where all bonds in the ring are formally single); b) a RAHB ring

RAHB rings are constituent elements of various materials and biomolecules and the non-covalent interactions, where they are involved, can be important for the design and function of these systems.[50-56] In the work presented here, we studied stacking interactions between RAHB and C_6 aromatic rings by analyzing all crystal structures in the Cambridge Structural Database and by performing quantum chemical calculations. To the best of our knowledge, this is the first systematic study on RAHB/C_6-aromatic stacking. RAHB/aromatic stacking interactions, studied in this work, are compared with previously studied stacking interactions of hydrogen-bridged rings,[39-41] in order to obtain a broader picture over stacking interactions of hydrogen-bridged species.

Methodology

A Cambridge Structural Database[57,58] (Version 5.39, November 2017 and updates) search is performed by using certain filters (3D coordinates determined; R factor not larger than 0.1; only non-disordered structures are included; no errors; no polymer or powder structures). Positions of hydrogen are normalized according to the criteria in the CSD (C-H 1.089 Å; N-H 1.015 Å; O-H 0.993 Å).

The criteria of the CSD search of fragments shown in Figure 2a include: D-A separation is set to be smaller than 4.0 Å; D-H-A angle is in the range from 90° to 180°; absolute torsion angles HDZY, DZYX and ZYXA are in the range from 0 to 10°. Structures with coordination number of D, Z, Y or X atoms larger than 3 or coordination number of the A atom larger than 2 and with absolute torsion angle StAXY (Figure 2b) that is not in the range between 160° and 180° are excluded from the analysis. This condition excludes structures with RAHB ring substituents that are not in the same plane as RAHB ring, since they can form additional side interactions, other than stacking, that would cause a contact to occur. Hydrogen donor (D) and acceptor (A) atoms can be only N, O or S atoms; all covalent bonds in RAHB ring were set to be acyclic, i.e. the RAHB ring is not fused with other rings. This condition is applied in order to avoid the stacked structures that would be the consequence of a contact between the fused ring and C_6-aromatic ring, instead of RAHB and C_6-aromatic rings. Contacts between RAHB and C_6-aromatic ring are defined by separation between two ring centers, d, not larger than 4.5 Å (Figure 2a). All fragments defined in this way are analyzed, regardless the size of the whole molecular structure that these fragments belong to.

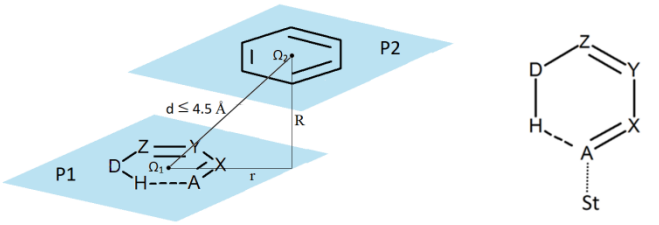

a) b)

Figure 2 a) RAHB ring/C_6-aromatic ring contacts studied by CSD search; Ω_1 and Ω_2 are RAHB and C_6-aromatic ring centers, respectively, r is the horizontal displacement between the ring centers, while R is the distance between the C_6-aromatic ring center and the RAHB ring plane, P1 and P2 (RAHB and C_6-aromatic ring planes, respectively) define dihedral angle P1/P2; b) RAHB ring with one substituent (St) on the acceptor atom (coordination number of A atom is 2). The dotted line indicates any bond type. The fragment StAXY forms torsion angle θ, of which the absolute value is in the range from 160° to 180°, i.e. the A-St bond is in the plane of RAHB ring.

Quantum chemical calculations were done by using Gaussian09 series of programs.[59] Model systems for the calculations were three systems consisted of a benzene molecule and a RAHB molecule that is chosen according to abundance in the CSD. The monomer optimizations were done by using the Møller-Plesset Perturbation Theory of Second Order (MP2) and Correlation-Consistent Polarized Valence-only Triple-zeta (cc-pVTZ) basis set. Single point interaction energies were calculated as differences between the whole system energies and the sum of the energies of the constituent molecules, with the counterpoise Basis Set Superposition Error (BSSE) correction.[60] All interaction energies calculated by the method of Coupled-Cluster with Single, Double and Perturbative Triple Excitations at Complete Basis Set (CCSD(T)/CBS) were obtained by extrapolation of Mackie and DiLabio.[61]

The potential energy curves were calculated by MP2/cc-pVTZ method, since it is in good agreement with CCSD(T)/CBS method (Tables S1-S5), that is considered gold standard in quantum chemistry.[62]

Maps of electrostatic potentials were calculated and visualized in Wavefunction Analysis-Surface Analysis Suite (WFA-SAS) program,[63] from the wave functions calculated in Gaussian09 at MP2/cc-pVTZ level.

The Symmetry-Adopted Perturbation Theory (SAPT) analysis[64] was performed at SAPT2+3/cc-pVQZ (Correlation-Consistent Polarized Valence-only Quadruple-zeta) level,[65] by using PSI4 program package.[66] In the SAPT analysis the total SAPT2+3 interaction energy is composed of electrostatic, exchange-repulsion, induction and dispersion terms. However, it should

be mentioned that no perfect separation between the total energy contributions is possible.[67] It is in accordance with the Hellmann-Feynman theorem[68,69] that describes non-covalent interactions as entirely Coulombic, with attractive contributions from the nucleus-electron interactions and repulsive contributions from the nucleus-nucleus interactions.

Results and discussion

Using criteria described in methodology section, 1122 structures were found with both six-membered RAHB and C_6-aromatic rings, present in any mutual orientation in the CSD. In these structures there are 677 contacts between these rings (Figure 2a), while parallel contacts (dihedral angle P1/P2, as defined in Figure 2a, smaller than 10°) are the most frequent type of contacts since 59.4% of contacts are parallel (Figure 3). There are only six contacts with P1/P2 angle of exactly 0.0°. The interplane separations are in the range from 3.0 to 4.0 Å (Figure 4), which is typical for stacking interactions.[2-7,18,19,39-41] No correlation between horizontal displacements and interplane separations is found (Figure S1), since determination coefficient is small (0.0171). An example of a RAHB/aromatic contact in a crystal structure is shown in Figure 5.

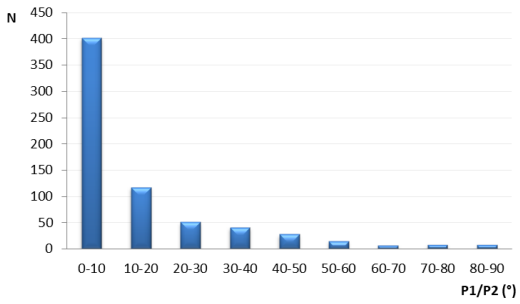

Figure 3. The distribution of dihedral angle between the planes of RAHB and C_6-aromatic rings that are found in the CSD.

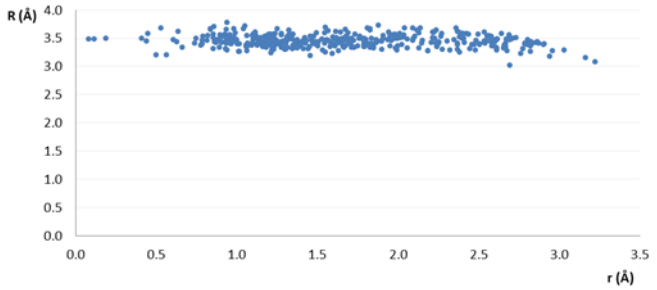

Figure 4. A scatterplot of the interplane separations and horizontal displacements of the centers of RAHB and C_6-aromatic rings, for parallel contacts found in the CSD.

RAHB ring atom sequences are analyzed and it was found that three types of RAHB rings are frequently present in RAHB/C_6-aromatic ring contacts: HNNCCO, HOCCCO and HNCCCO sequences (Table 1). These three types of the rings are 85% of all RAHB rings that form RAHB/C_6-aromatic ring contacts. Because of the frequent presence, these three rings, molecules shown in Figure 6, were used as model systems for quantum chemical calculations. To additionally show that the choice of model systems is appropriate, we analyzed dihedral angle distributions and a scatterplot of interplane separations and horizontal displacements of RAHB/C_6-aromatic contacts in case of HNNCCO, HOCCCO and HNCCCO RAHB ring atom sequences separately (Figures S2 and S3). Since these data show trends that are similar to overall trends (Figures 3 and 4), we used these molecules as model systems (Figure 6).

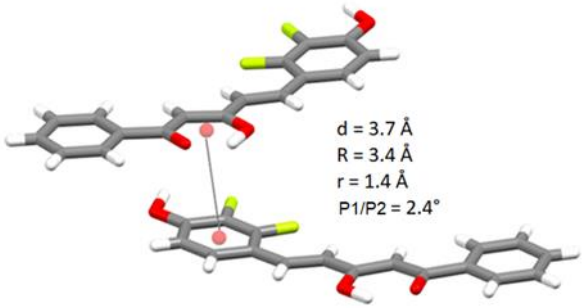

Figure 5. An example of a RAHB/C_6-aromatic contact from CSD (refcode DIVGUN) with geometrical parameters as labelled in Figure 2a.

Table 1. The most frequent RAHB ring atom sequences, found in RAHB ring/C_6-aromatic contacts in CSD and relative abundances of every particular group.

The RAHB ring composition (HDZYXA, Figure 1)	Number of contacts (percentage) from the total number of stacking contacts
HNNCCO	147 (36.6%)
HOCCCO	130 (32.3%)
HNCCCO	67 (16.7%)

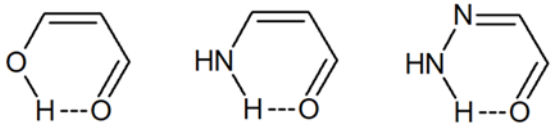

a) b) c)

Figure 6. Three molecules chosen for the calculation of RAHB/benzene interaction energies; a) malonaldehyde ($H_4C_3O_2$); (b) its mononitrogen analog (H_5C_3NO) and (c) its dinitrogen analog ($H_4C_2N_2O$).

Several quantum chemical methods, including MP2 and some D3 dispersion corrected[70] Density Functional Theory (DFT-D3) methods and basis sets were used for the calculation of RAHB/benzene interaction energies, for selected model systems in various orientations (Figure S4, Tables S1-S5). Some general conclusions could be drown about the performances of the chosen methods. MP2 method gives good results (in agreement with CCSD(T)/CBS) only at cc-pVTZ level, since relative errors are mostly under 10%. BLYP-D3 method also gives acceptable results for most systems, with somewhat higher relative errors (up to 21%). Few functionals (TPSS, BP86, PBE1PBE, M05) are relatively good for the calculations in all geometries except sandwich. A general trend can be observed

in case of M06 functional, since the results are better with smaller basis sets. At the other side, M052X functional gives better results by using larger basis sets. Since MP2/cc-pVTZ level gives results in good agreement with CCSD(T)/CBS (Figure S4, Tables S1-S5), we used it to calculate potential energy curves.

Potential energy curves were calculated for benzene/RAHB ring systems in parallel alignment by moving benzene molecule along Ω_1-C direction and the orthogonal direction in the RAHB ring plane (Figure 7) and varying distances between the ring planes for every particular offset value, while the monomer geometries were fixed. The curves are plotted as dependences of interaction energies on horizontal displacements at optimal distances between the ring planes. All calculated curves have two minima, with the exception of the curve obtained for $H_4C_3O_2$/benzene stacking interaction along Ω_1-C direction (Figure 8a). The lowest minima at curves along Ω_1-C direction (Figure 8a) are at negative offset values; at -1.4 Å, -1.5 Å and -1.4 Å, for $H_4C_3O_2$/benzene, H_5C_3NO/benzene and $H_4C_2N_2O$/benzene, respectively. The minima at positive offset values are at 1.0 Å for H_5C_3NO/benzene and $H_4C_2N_2O$/benzene, while the curve obtained for $H_4C_3O_2$/benzene interaction is almost flat in the region of offset values between 0.5 and 1.5 Å. Along the orthogonal direction (Figure 8b), the lower minima correspond to positive offset (1.5 Å) for $H_4C_3O_2$/benzene interaction and to negative offset (-1.8 Å) for H_5C_3NO/benzene interaction. For $H_4C_2N_2O$/benzene system two minima (at -1.6 Å and 1.5 Å) have similar energy. Thus, all minima geometries correspond to parallel-displaced arrangement. The calculated distances between parallel ring planes are all in the range between 3.0 and 4.0 Å (Figure S5), in accordance with the results from CSD search (Figure 4).

Interaction energies at CCSD(T)/CBS level, calculated for the lowest energy minima at each potential curve, are in the relatively small range, from -2.89 to -3.54 kcal/mol (Figure 9). The strongest interaction is in $H_4C_3O_2$/benzene system along Ω_1-C direction, with interaction energy of -3.54 kcal/mol, followed by H_5C_3NO/benzene system along direction orthogonal to Ω_1-C, with interaction energy of -3.47 kcal/mol. The weakest interaction is in $H_4C_2N_2O$/benzene system, -2.89 kcal/mol.

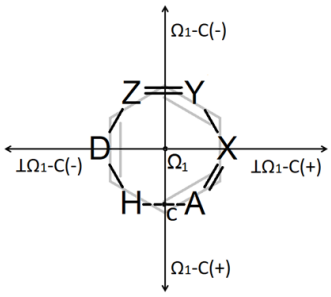

Figure 7. A schematic representation of the two directions for calculating potential energy curves for RAHB/benzene stacking interactions; Ω_1-C and the orthogonal direction-$\perp\Omega_1$-C in the RAHB ring plane. Positive and negative values of horizontal displacements are indicated.

Previously studied RAHB/RAHB dimers[41] are found to be more stable than RAHB/benzene systems in case of $H_4C_3O_2$ and H_5C_3NO. Namely, the most stable interactions of $H_4C_3O_2/H_4C_3O_2$ and H_5C_3NO/H_5C_3NO dimers have interaction energies of -4.26 and -4.74 kcal/mol, respectively.[41] while stacking interaction energies of $H_4C_3O_2$/benzene and H_5C_3NO/benzene systems are -3.54 and -3.47 kcal/mol, respectively (Figure 9). On the other hand, $H_4C_2N_2O/H_4C_2N_2O$ stacking interaction (-2.23 kcal/mol),[41] is weaker than $H_4C_2N_2O$/benzene interaction (-3.20 kcal/mol, Figure 9). The calculated RAHB/benzene stacking interactions are weaker than mutual interactions of saturated five-membered hydrogen-bridged rings (-4.9 kcal/mol),[39] as well as the interactions between saturated five-membered hydrogen-bridged rings and C_6-aromatic rings (-4.4 kcal/mol).[40]

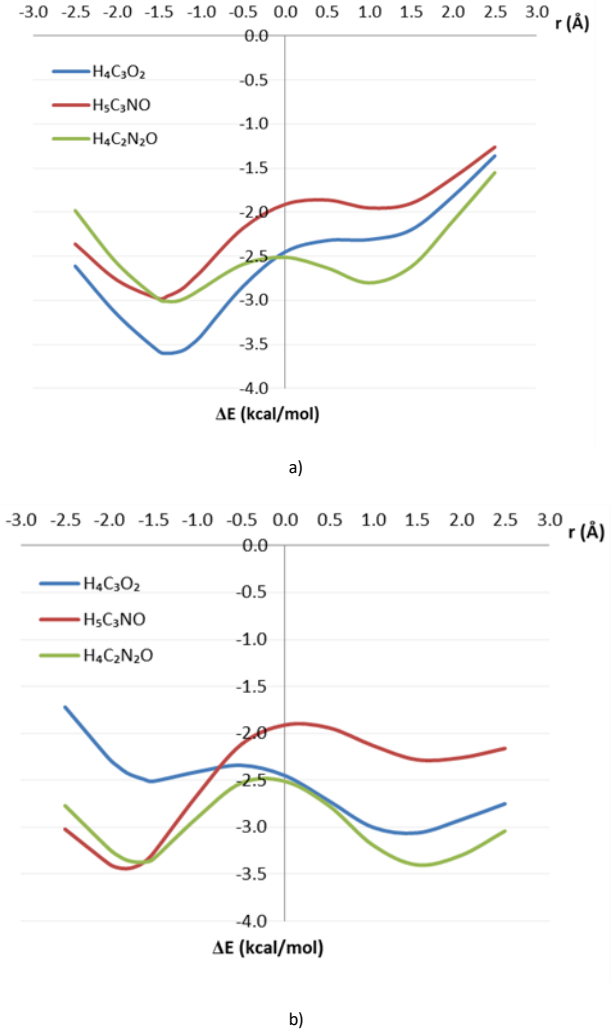

Figure 8. Potential energy curves calculated at MP2/cc-pVTZ level, at optimal ring separations for every particular offset value, for stacking in benzene/RAHB ring systems a) along Ω_1-C direction; b) along the direction orthogonal to Ω_1-C in the RAHB ring plane (Figure 7).

However, interaction energies in all RAHB/benzene systems calculated in this work (Figure 9) are stronger than benzene/benzene stacking interaction (-2.73 kcal/mol),[47]

although slightly weaker than pyridine/pyridine stacking interaction (-3.84 kcal/mol, or -4.00 kcal/mol, depending on the method used)[71] It should, however, be mentioned that benzene system is more stable in T-shaped than parallel-stacked form,[72] while stacked sandwich geometries are frequently found in heterocyclic crystal structures.[1,73]

Geometries of RAHB/benzene systems are optimized at MP2/cc-pVTZ level by using geometries corresponding to the potential curves minima (Figure 9) as starting geometries, while the energies of the optimized structures were recalculated at CCSD(T)/CBS level (Table S6 and Figure S6). The optimized geometries of $H_4C_3O_2$/benzene minima obtained in both directions and H_5C_3NO/benzene and $H_4C_2N_2O$/benzene minima obtained along Ω_1-C direction are almost parallel (with angle between rings less than 5.5°), while the optimized geometries of H_5C_3NO/benzene and $H_4C_2N_2O$/benzene minima obtained in the direction orthogonal to Ω_1-C direction are not parallel. Namely, in H_5C_3NO/benzene dimer the angle between the ring planes is 13.71°, while in $H_4C_2N_2O$/benzene the angle between the ring planes is 14.08° (Figure S6). The optimized geometries that kept (almost) parallel orientations after the geometry optimization have only slightly stronger interaction energies than non-optimized systems; they are up to 0.7 kcal/mol more stable than geometries at the potential curves minima. However, the interactions of the non-parallel optimized geometries are significantly stronger, namely the calculated interaction energies are -4.42 kcal/mol for H_5C_3NO/benzene system and -4.15 kcal/mol for $H_4C_2N_2O$/benzene system (Table S6, Figure S6).

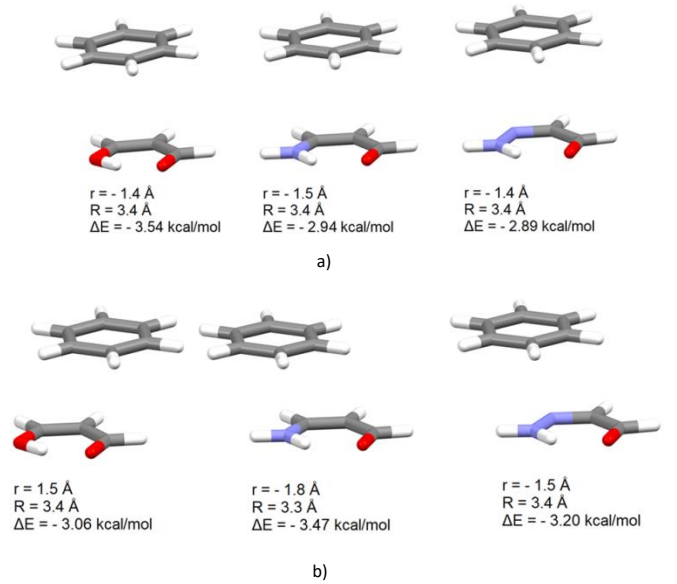

Figure 9. Geometries of the lowest energy potential curves minima a) $H_4C_3O_2$/benzene, H_5C_3NO/benzene and $H_4C_2N_2O$/benzene systems along Ω_1-C direction; b) $H_4C_3O_2$/benzene, H_5C_3NO/benzene and $H_4C_2N_2O$/benzene systems along the direction orthogonal to Ω_1-C, with geometric parameters (Figure 2a) and CCSD(T)/CBS interaction energies (ΔE), obtained by the extrapolation method of Mackie and DiLabio[61].

It is interesting that H-O distances were changed in optimized RAHB/benzene systems, compared to the optimized monomer geometries (Figure S6). In the optimized structures, where stacked arrangement is preserved (P1/P2 angle smaller than 10°), there is a small shortening of H-O bonds. This effect is already observed in our previous study about stacking interactions of RAHB rings[41] and also in clusters of picolinic acid N-oxide.[74] The H-O distances increase in optimized systems where stacked arrangement is not preserved (Figure S6).

The SAPT analysis was performed at SAPT2+3/cc-pVQZ level, which is in good agreement with CCSD(T)/CBS method (Figures 9 and 10). The results show that the largest attractive contribution to the total interaction energies is dispersion. However, repulsive exchange is also very large, hence the net dispersion (the sum of dispersion and exchange-repulsion terms[68,75]) is quite small, less than 1.0 kcal/mol. Hence, the electrostatic terms are larger than net dispersion terms in all systems (Figure 10), similar to our previous work on $H_4C_3O_2/H_4C_3O_2$ and H_5C_3NO/H_5C_3NO interactions.[41] The electrostatic contribution is smaller in $H_4C_2N_2O$/benzene systems, compared to $H_4C_3O_2$/benzene and H_5C_3NO/benzene systems, but it is more dominant than in previous results on $H_4C_2N_2O/H_4C_2N_2O$ dimer, where electrostatics and net dispersion terms are almost equal.[41] Induction term also contributes to attraction, it is close to -1.0 kcal/mol for most geometries, and with one exception of $H_4C_2N_2O$/benzene, it is always more attractive than net dispersion (Figure 10).

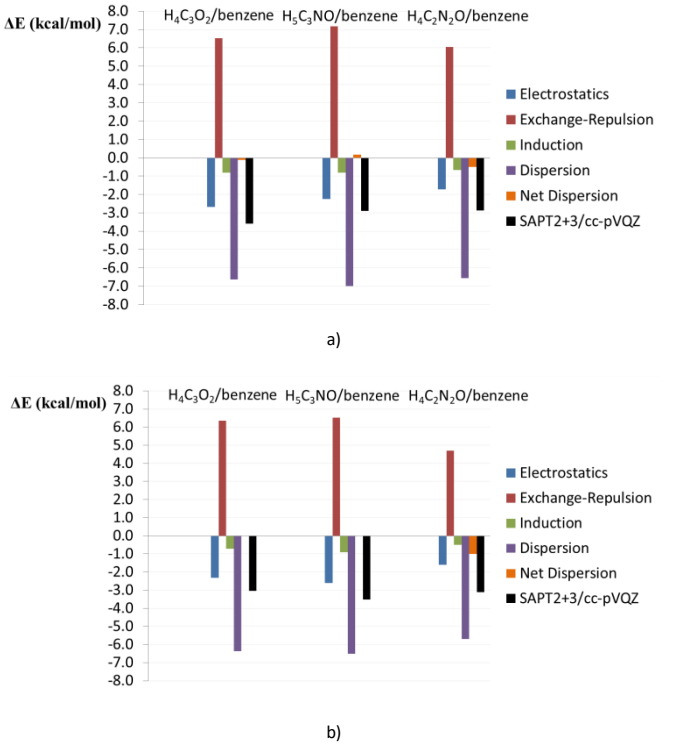

Figure 10. SAPT2+3/cc-pVQZ energy decomposition analysis of three stacking RAHB/benzene systems. The total SAPT2+3 interaction energy is composed of electrostatic, exchange-repulsion, induction and dispersion terms. Net dispersion is a sum of dispersion and exchange-repulsion terms. [68,72] a) the minima along Ω_1-C direction (Figure 9a); b) the minima along the direction orthogonal to Ω_1-C (Figure 9b) Net dispersion energy values are negligible in $H_4C_3O_2$/benzene and H_5C_3NO/benzene systems along Ω_1-C direction and equal to zero in $H_4C_3O_2$/benzene system in the orthogonal direction.

Since electrostatic contribution is the most important, the geometries of the minima can be explained by electrostatic potential maps (Figure 11). The relevance of electrostatic potential maps in the non-covalent interaction studies is intuitively convincing, since the regions of electrostatic potentials of the opposite sign tend to be located in the close proximity. [68,69] Furthermore, interaction energies were successfully reproduced using the electrostatic potential maxima and minima values of the interacting regions as the only input parameters.[76]

The geometries of energy minima correspond to an overlay of oppositely charged electrostatic potential regions; namely, benzene ring center, with negative electrostatic potential, overlays the regions of positive electrostatic potentials of RAHB molecules (Figures 9 and 11).

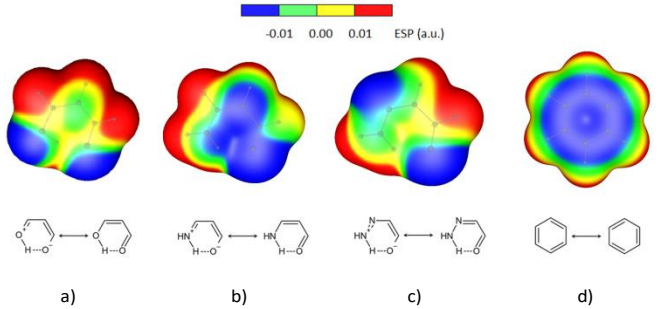

Figure 11. The electrostatic potential maps of the molecules used for quantum chemical calculations; a) $H_4C_3O_2$; b) H_5C_3NO; c) $H_4C_2N_2O$ and d) benzene molecule

The interaction energy calculations were also performed on a set of randomly chosen stacking contacts from the CSD. The positions of RAHB and C_6-aromatic rings were exactly the same as in the CSD, without any geometry optimizations (Figure S7). All substituents that were present in these structures were replaced by hydrogen atoms, by keeping all valence and torsion angles unchanged, while setting bond lengths to be identical to those in the corresponding optimized RAHB rings. Some of the RAHB ring atom sequences were in some cases those that were used for the potential energy curves calculations (HNNCCO, HOCCCO and HNCCCO), but also some of the others (HNCCCN, HNCCNN, HNNCCN, HNNCNN and HOCCCS). The range of interaction energies obtained by potential energy curves calculations (Figure 8) corresponds to the range of interaction energies obtained for the CSD geometries (Table S7), since the energies are roughly between -1.2 kcal/mol and -3.6 kcal/mol, with two exceptions, PUVCOA (HNNCNN) and NIZKOX (HOCCCS), where the interactions are stronger, with the calculated interaction energies of -3.98 kcal/mol (Table S7).

Conclusions

Stacking arrangement of the six-membered RAHB and C_6-aromatic rings is present in 59.4% of contacts between these two ring types in CSD. The most abundant RAHB rings that form stacked contacts with C_6-aromatic rings are those with HOCCCO, HNCCCO, and HNNCCO ring atom sequences. They are present in 32.3%, 16.7%, and 36.6% of all stacked contacts, respectively. Thus, quantum chemical calculations are performed using parallel $H_4C_3O_2$/benzene, H_5C_3NO/benzene and $H_4C_2N_2O$/benzene model systems. The minima on calculated potential energy curves show that the most stable interaction geometries all correspond to parallel-displaced orientations. The strongest calculated single point interaction energies at CCSD(T)/CBS level are -3.54 kcal/mol for $H_4C_3O_2$/benzene, -3.47 kcal/mol for H_5C_3NO/benzene and -3.20 kcal/mol for $H_4C_2N_2O$/benzene, while the most stable optimized stacked structure corresponds to $H_4C_3O_2$/benzene system, with interaction energy of -3.73 kcal/mol. The RAHB/benzene interactions can be weaker (in case of $H_4C_3O_2$ and H_5C_3NO molecules) or stronger (in case of $H_4C_2N_2O$ molecule) than RAHB/RAHB interactions. The energy decomposition analysis at SAPT2+3/cc-pVQZ level shows that electrostatic component is the most dominant contribution to the interaction energies in all systems, since dispersion contribution is almost or completely canceled by exchange-repulsion term. The most stable geometries can be explained by electrostatic potential maps, since there is the overlay of the regions of electrostatic potential of the opposite sign.

Conflicts of interest

There are no conflicts to declare.

Acknowledgements

This work was supported by the Serbian Ministry of Education, Science and Technological Development (Grant 172065) and an NPRP grant from the Qatar National Research Fund (a member of the Qatar Foundation) (grant number NPRP8-425-1-087).

Notes and references

1 L. M. Salonen, M. Ellermann, F. Diederich, *Angew. Chem. Int. Ed.,* 2011, **50**, 4808.
2 C. Janiak, *J. Chem. Soc. Dalton Trans*., 2000, **21**, 3885.
3 D. B. Ninković, G. V. Janjić, D. Ž. Veljković, D. N. Sredojević, S. D. Zarić, *ChemPhysChem,* 2011, **12**, 3511.
4 T. Janowski, P. Pulay, *Chem. Phys.Lett*.,2007, **447**, 27.
5 M. O. Sinnokrot, C. D. Sherrill, *J. Phys. Chem. A*, 2006, **110**, 10656.
6 R. Podeszwa, R. Bukowski, K. Szalewicz, *J. Phys. Chem. A*, 2006, **110**, 10345.
7 D. B. Ninković, J. M. Andrić, S. D. Zarić, *ChemPhysChem*, 2013, **14**, 237.
8 D. Yang, S. Gao, Y. Fang, X. Lin, X. Jin, X. Wang, L. Ke, K. Shi, *Nanomedicine-UK*, 2018, **13**, 3159.
9 M. M. Rahman, Z. T. Muhseen, M. Junaid, H. Zhang, *Curr Protein Pept Sc,* 2015, **16** , 502.
10 K. Watanabe, K. Akagi, *Sci Technol Adv Mater*., 2014, **15**, 044203.
11 S. Grimme, *Angew. Chemie - Int. Ed.,* 2008, **47**, 3430.

12 D. B. Ninković, D. Z. Vojislavljević-Vasilev, V. B. Medaković, M. B. Hall, E. N. Brothers, S. D. Zarić, *Phys. Chem. Chem. Phys*., 2016, **18**, 25791.
13 E. M. Cabaleiro-Lago, J. Rodríguez-Otero, *ChemistrySelect*, 2017, **2**, 5157.
14 H. Gunaydin, M. D. Bartberger, *ACS Med. Chem. Lett.,* 2016, **7**, 341.
15 M. Alonso, T. Woller, F. J. Martín-Martínez, J. Contreras-García, P. Geerlings, F. De Proft, *Chem-Eur. J.,* 2014. **20**, 4931.
16 K. Yuan, R.-S. Zhao, J.-J. Zheng, H. Zheng, S. Nagase, S.-D. Zhao, Y.-Z. Liu, X. Zhao, *J. Comput. Chem*., 2017, **38**, 730.
17 J. W. G. Bloom, S. E. Wheeler, *Angew. Chemie - Int. Ed.,* 2011, **50**, 7847.
18 I. S. Antonijević, D. P. Malenov, M. B. Hall, S. D. Zarić, *Acta Cryst.,* 2019, **B75**, 1.
19 D. P. Malenov, G. V. Janjić, V. B. Medaković, M. B. Hall, S. D. Zarić, *Coord. Chem. Rev.,* 2017, **345**, 318.
20 E. Craven, C. Zhang, C. Janiak, G. Rheinwald, H. Lang, *Z. Anorg. Allg. Chem.,* 2003, **629**, 2282.
21 A. P. McKay, W. K. C. Lo, D. Preston, G. I. Giles, J. D. Crowley, J. E. Barnsley, K. C. Gordon, D. A. McMorran, *Inorg. Chim. Acta,* 2016, **446**, 41.
22 P. P. Chakrabarty, D. Biswas, S. García-Granda, A. D. Jana, S. Saha, *Polyhedron,* 2012, **35**, 108.
23 D. Biswas, P. P. Chakrabarty, S. Saha, A. D. Jana, D. Schollmeyer, S. García-Granda, *Inorg. Chim. Acta,* 2013, **408**, 172.
24 S. Jana, S. Khan, A. Bauzá, A. Frontera, S. Chattopadhyay, *J. Mol. Struct.,* 2017, **1127**, 355.
25 S. Bhattacharya, S. Roy, K. Harms, A. Bauza, A. Frontera, S. Chattopadhyay, *Inorg. Chim. Acta,* 2016, **442**, 16.
26 G. Mahmoudi, A. Castiñeiras, P. Garczarek, A. Bauzá, A. L. Rheingold, V. Kinzhybalo, A. Frontera, *CrystEngComm,* 2016, **18**, 1009.
27 G. Mahmoudi, A. Bauzá, A. V. Gurbanov, F. I. Zubkov, W. Maniukiewicz, A. Rodríguez-Diéguez, E. López-Torres, A. Frontera, *CrystEngComm,* 2016, **18**, 9056.
28 J. Pasán, J. Sanchiz, C. Ruiz-Pérez, F. Lloret, M. Julve, *Eur. J. Inorg. Chem*., 2004, **2004**, 4081.
29 A. Sousa-Pedrares, J. A. Viqueira, J. Antelo, E. Labisbal, J. Romero, A. Sousa, O. R. Nascimento, J. A. García-Vázquez, *Eur. J. Inorg. Chem.,* 2011, **2011**, 2273.
30 X. Ren, J. Xie, Y. Chen, R. K. Kremer, *J. Mol. Struct*., 2003, **660**, 139.
31 J. L. Liu, Q. Liu, Y. X. Sui, B. Q. Yao, X. M. Ren, H. Zhang, H. B. Duan, Q. Meng, *J. Inorg. Chem. Commun.,* 2010, **13**, 786.
32 D. P. Malenov, S. D. Zarić, *Dalton Trans*., 2019, **48**, 6328.
33 J. P. Blagojević Filipović, M. B. Hall, S. D. Zarić, *Adv. Inorg. Chem.*,2019, **73**, 159.
34 G. Mahmoudi, J. K. Zaręba, A. Bauzá, M. Kubicki, A. Bartyzel, A. D. Keramidas, L. Butusov, B. Mirosław, A. Frontera, *CrystEngComm,* 2018, **20**, 1065.
35 F. A. Afkhami, A. A. Khandar, G. Mahmoudi, W. Maniukiewicz, A. V. Gurbanov, F. I. Zubkov, O. Şahin, O. Z. Yesilel, A. Frontera, *CrystEngComm,* 2017, **19**, 1389.
36 Y. P. Singh, R. N. Patel, Y. Singh, D. Choquesillo-Lazarte, R. J. Butcher, *Dalton Trans*., 2017, **46**, 2803.
37 E. R. T. Tiekink, *Coord. Chem. Rev.,* 2017, **345**, 209.
38 E. N. M. Yusof, N. M. Nasri, T. B. S. A. Ravoof, E. R. T. Tiekink, *Molbank,* 2019, **2019**, M1057.
39 J. P. Blagojević, S. D. Zarić, *Chem. Commun.,* 2015, **51**, 12989.
40 J. P. Blagojević, D. Ž. Veljković, S. D. Zarić, *CrystEngComm,* 2017, **19**, 40.
41 J. P. Blagojević Filipović, M. B. Hall, S. D. Zarić, *Cryst. Growth Des*, 2019, **19**, 5619.
42 H. Karabiyik, H. Karabiyik, N. Ocak Iskeleli, *Acta Cryst*., 2012, **B68**, 71.
43 Z. Yang, C. Ge, J. Liu, Y. Chong, Z. Gu, C. A. Jimenez-Cruz, Z. Chai, R. Zhou, Nanoscale, 2015, 7, 18725.
44 M. Li, B. Wang, X. An, Z. Li, H. Zhu, B. Mao, D. G. Calatayud, T. D. James, Dyes Pigments, 2019, 170, 107476.
45 E.-J. Gao, J. Chen, Y. Hui, S. Wu, T. Zhang, D. Song, D. Liu, M.-C. Zhu, Inorg. Chem. Commun., 2019, 107, 107488.
46 S. Rajesh, A. B. Bose, ACS Appl. Mater. Inter., 2019, 11, 27706.
47 E. C. Lee, D. Kim, P. Jurecka, P. Tarakeshwar, P. Hobza, K. S. Kim, *J. Phys. Chem. A*, 2007, **111**, 3446.
48 K. S. Kim, S. Karthikeyan, N. J. Singh, *J. Chem. Theory Comput.,* 2011, **7**, 3471.
49 C. I. Yeo, S. N. A. Halim, S. W. Ng, S. L. Tan, J. Zukerman-Schpector, M. A. B. Ferreira, E. R. T. Tiekink, *Chem. Commun*., 2014, **50**, 5984.
50 K. T. Mahmudov, A. J. L. Pombeiro, *Chem. Eur. J.,* 2016, **22**, 16356.
51 K. T. Mahmudov, M. N. Kopylovich, M. F. C. Guedes da Silva, A. J. L. Pombeiro, *Coord. Chem. Rev.,* 2017, **345**, 54.
52 K. T. Mahmudov, A. V. Gurbanov, F. I. Guseinov, M. F. C. Guedes da Silva, *Coord. Chem. Rev.,* 2019, **387**, 32.
53 P. Majewska, M. Rospenk, B. Czarnik-Matusewicz, L. Sobczyk, *Chem. Phys. Lett*., 2009, **473**, 75.
54 G. Gilli, P. Gilli, *The Nature of the Hydrogen Bond*; Oxford University Press, 2009.
55 X. Su, S. Voskian, R. P. Hughes, I. Aprahamian, *Angew. Chem. Int. Ed.,* 2013, **52**, 10734.
56 K. Kanosue, T. Shimosaka, J. Wakita, S. Ando, *Macromolecules,* 2015, **48**, 1777.
57 F. H. Allen, *Acta Cryst.,* 2002, **B58**, 380.
58 C. R. Groom, I. J. Bruno, M. P. Lightfoot, S. C. Ward, *Acta Cryst.,* 2016, **B72**, 171.
59 M. J. Frisch, G. W. Trucks, H. B. Schlegel, G. E. Scuseria, M. A. Robb, J. R. Cheeseman, G. Scalmani, V. Barone, G. A. Petersson, H. Nakatsuji, et al. *Gaussian 09, Revision D.01*. 2016.
60 S. F. Boys, F. Bernardi, *Mol. Phys.,* 1970, **19**, 553.
61 I. D. Mackie, G. A. DiLabio, *J. Chem. Phys.,* 2011, **135**, 134318.
62 M. O. Sinnokrot, E. F. Valeev, C. D. Sherrill, *J. Am. Chem. Soc*., 2002, **124**, 10887.
63 F. A. Bulat, A. Toro-Labbé, T. Brinck, J. S. Murray, P. Politzer, *J. Mol. Model.,* 2010, **16**, 1679.
64 B. Jeziorski, R. Moszynski, K. Szalewicz, *Chem. Rev.,* 1994, **94**, 1887.
65 E. G. Hohenstein, C. D. Sherrill, *J. Chem. Phys.,* 2010, **133**, 014101.
66 R. M. Parrish, L. A. Burns, D. G. A. Smith, A. C. Simmonett, A. E. DePrince, E. G. Hohenstein, U. Bozkaya, A. Y. Sokolov, R. Di Remigio, R. M. Richard, J. F. Gonthier, A. M. James, H. R. McAlexander, A. Kumar, M. Saitow, X. Wang, B. P. Pritchard, P. Verma, H. F. Schaefer, K. Patkowski, R. A. King, E. F. Valeev, F. A. Evangelista, J. M. Turney, T. D. Crawford, C. D. Sherrill, *J. Chem. Theory Comput.,* 2017, **13**, 3185.

67 T. Clark, J. S. Murray, P. Politzer, Phys. Chem. Chem. Phys., 2018, 20, 30076.
68 R. P. Feynman, Phys. Rev., 1939, 56, 340.
69 H. Hellmann, Einführung in die Quantenchemie, Deuticke, Leipzig, 1937, p. 285.
70 S. Grimme, J. Antony, S. Ehrlich, H. Krieg, J. Chem. Phys., 2010, 132, 154104.
71 E. G. Hohenstein, C. D. Sherrill, J. Phys. Chem. A, 2009, 113, 878.
72 C. R. Martinez, B. L. Iverson, Chem. Sci., 2012, 3, 2191.
73 C. Jelsch, K. Ejsmont, L. Huder, IUCrJ, 2014, 1, 119.
74 J. Panek, J. Stare, D. Hadži, *J. Phys. Chem. A,* 2004, **108**, 7417.
75 C. D. Sherrill, *Acc. Chem. Res.,* 2013, **46**, 1020.
76 J. S. Murray, Z. Peralta-Inga Shields, P. G. Seybold, P. Politzer, J. Comput. Sci., 2015, 10, 209.